

See discussions, stats, and author profiles for this publication at: <https://www.researchgate.net/publication/260128774>

# Anomalous Trapped Exciton and d-f Emission in $\text{Sr}_4\text{Al}_{14}\text{O}_{25}:\text{Eu}(2+)$

ARTICLE in THE JOURNAL OF PHYSICAL CHEMISTRY A · FEBRUARY 2014

Impact Factor: 2.69 · DOI: 10.1021/jp500947q · Source: PubMed

CITATIONS

9

READS

207

## 4 AUTHORS:



**Danuta Dutczak**

University of Tuebingen

25 PUBLICATIONS 110 CITATIONS

SEE PROFILE



**Cees Ronda**

Philips

127 PUBLICATIONS 2,787 CITATIONS

SEE PROFILE



**Thomas Jüstel**

Fachhochschule Münster

356 PUBLICATIONS 3,101 CITATIONS

SEE PROFILE



**Andries Meijerink**

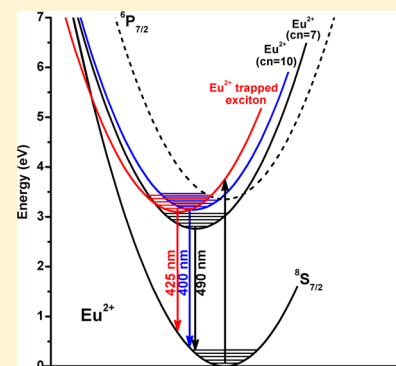
Utrecht University

364 PUBLICATIONS 13,485 CITATIONS

SEE PROFILE

Anomalous Trapped Exciton and d–f Emission in  $\text{Sr}_4\text{Al}_{14}\text{O}_{25}:\text{Eu}^{2+}$ Danuta Dutczak,<sup>†,‡</sup> Cees Ronda,<sup>‡,§</sup> Thomas Jüstel,<sup>†</sup> and Andries Meijerink<sup>\*,‡</sup><sup>†</sup>Department of Chemical Engineering, Münster University of Applied Sciences, Stegerwaldstr. 39, D-48565 Steinfurt, Germany<sup>‡</sup>CML, Debye Institute for Nanomaterials Science, Utrecht University, 3508 TA, Utrecht, The Netherlands<sup>§</sup>Philips Research Laboratories—Eindhoven, High Tech Campus 4, 5656 AE, Eindhoven, The Netherlands

**ABSTRACT:** The photoluminescence and time-resolved emission for  $\text{Eu}^{2+}$  in  $\text{Sr}_4\text{Al}_{14}\text{O}_{25}$  has been investigated in the temperature range 4 to 500 K. The  $\text{Eu}^{2+}$  emission changes in a peculiar way with temperature. At low temperature two emission bands are observed at 490 and 425 nm, which are attributed to emission from  $\text{Eu}^{2+}$  on the 7- and 10-coordinated sites. Upon raising the temperature, an unexpectedly large blue shift to 400 nm is observed for the 425 nm emission band. To explain these observations, the 400 and 425 nm emission bands are assigned to d–f and trapped exciton emission, for  $\text{Eu}^{2+}$  on the 10-coordinated site. The trapped exciton emission is characterized by a short (0.5  $\mu\text{s}$ ) decay time. The temperature dependence of the emission is explained by a configurational coordinate diagram in which the  $\text{Eu}^{2+}$  trapped exciton state is at a slightly lower energy than the lowest energy  $4f^65d$  state. Upon raising the temperature, the  $4f^65d$  state is thermally populated and emission from this state is observed, and because of the smaller lattice relaxation (smaller Stokes shift), a large blue shift from 425 to 400 nm is observed.



## 1. INTRODUCTION

The luminescence of  $\text{Eu}^{2+}$  in alkaline earth aluminates has been studied extensively, especially for application as blue or green phosphor in fluorescent tubes.<sup>1,2</sup> A relatively new composition is  $\text{Sr}_4\text{Al}_{14}\text{O}_{25}:\text{Eu}^{2+}$ , which was first reported in the 1980s as fluorescent tube phosphor.<sup>3</sup> The phosphor shows an intense emission band around 490 nm, which was assigned to  $4f^65d \rightarrow 4f^7$  (d–f) emission for  $\text{Eu}^{2+}$  in one of the two crystallographic sites available for  $\text{Eu}^{2+}$  in this host lattice. A weak band around 400 nm was also observed and assigned to  $\text{Eu}^{2+}$  d–f emission for  $\text{Eu}^{2+}$  in the other crystallographic site. The low relative intensity of the higher energy emission band was explained by energy transfer from the high energy site to the low energy site at the concentrations applied, typically around 1 mol %. In later work the phosphor was discussed in relation to application in white light LEDs, and the emission spectra showing a 400 and 490 nm emission band were confirmed.<sup>4</sup> About 10 years ago, intense afterglow was reported for  $\text{Sr}_4\text{Al}_{14}\text{O}_{25}:\text{Eu}^{2+}$  codoped with  $\text{Dy}^{3+}$ , and research on the luminescence of this composition intensified.<sup>5–10</sup> In addition to the 400 and 490 nm emission band, also 425 nm emission was reported, but not explained.<sup>6</sup> In a recent paper by Nakazawa et al., careful temperature-dependent emission spectra were reported for  $\text{Sr}_4\text{Al}_{14}\text{O}_{25}$  doped with 0.5%  $\text{Eu}^{2+}$ .<sup>9</sup> Because of the lower  $\text{Eu}^{2+}$  concentration, the relative intensity of the 400 nm emission band is stronger (less energy transfer). Also, emission spectra at 90 K were reported. A clear redshift of the 400 nm emission band to 425 nm was observed upon cooling, but the shift was not explained. In this article, we aim to explain the peculiar behavior of the 400 nm  $\text{Eu}^{2+}$  emission band in  $\text{Sr}_4\text{Al}_{14}\text{O}_{25}:\text{Eu}^{2+}$ . On the basis of temperature-dependent emission spectra and luminescence lifetime measurements, we can assign the 400 nm

emission to normal d–f emission and the 425 emission to anomalous  $\text{Eu}^{2+}$  trapped exciton emission.

## 2. EXPERIMENTAL SECTION

**2.1. Synthesis.** The  $\text{Sr}_4\text{Al}_{14}\text{O}_{25}:\text{Eu}^{2+}$  samples were synthesized by a solid state method. Strontium carbonate (99.8% Dr. Paul Lohmann, Inc.), aluminum oxide (99.9% Degussa), and europium oxide (99.99% Treibacher) were used as starting materials. Small quantities of boric acid were used as a flux (5 mol % with respect to total number of mols of  $\text{Sr}_4\text{Al}_{14}\text{O}_{25}:\text{Eu}^{2+}$ ). The mixed powders were first precalcined at 1000 °C in air during 4 h. The second calcination was performed in a strongly reducing atmosphere comprising 30%  $\text{N}_2$  and 70%  $\text{H}_2$  at 1400 °C for 4 h.

**2.2. Characterization.** The crystallinity was checked by X-ray powder diffraction, and all samples were found to be single phase and in perfect agreement with the ICSD reference #88527 indicating that crystalline second phases are below the XRD detection limit of ~2%. Luminescence spectra were recorded on an Edinburgh FLS920 spectrofluorometer equipped with an Oxford Instruments helium flow cryostat for measurements down to 4 K. Luminescence lifetime measurements were performed using a pulsed (~10 ns) excimer (Lambda Physik LPX100) pumped dye laser (Lambda Physik LPD3000) in combination with a 1 GHz digital oscilloscope (Tektronix). The high resolution VUV spectroscopy measurements were carried out at the SUPERLUMI station of HASYLAB (DESY, Germany), using synchrotron

Received: February 1, 2014

Published: February 9, 2014

radiation from the DORIS III storage ring as excitation source.<sup>11</sup>

### 3. RESULTS AND DISCUSSION

The  $\text{Sr}_4\text{Al}_{14}\text{O}_{25}$  host crystallizes in an orthorhombic crystal structure with space group  $P_{nma}$ .<sup>12</sup> The structure consists of two layers made up of  $\text{AlO}_6$  octahedra separated by a double layer of  $\text{AlO}_4$  tetrahedra.<sup>4,13,14</sup> According to the structure, two different strontium sites with coordination numbers 10 and 7 exist in the  $\text{Sr}_4\text{Al}_{14}\text{O}_{25}$ . Because of the similar ionic radius,  $\text{Eu}^{2+}$  ions replace  $\text{Sr}^{2+}$  ions leading to two different types of luminescent  $\text{Eu}^{2+}$  centers. One can expect that the covalency and crystal field strength are stronger for the 7-fold coordinated site than for the 10-fold site, leading to a lower energy of the lowest crystal-field component of the  $[\text{Xe}]4f^65d^1$  configuration for  $\text{Eu}^{2+}$  on this site.

Figure 1 shows the VUV excited emission spectrum of undoped  $\text{Sr}_4\text{Al}_{14}\text{O}_{25}$  at 300 K. The spectrum is dominated by a

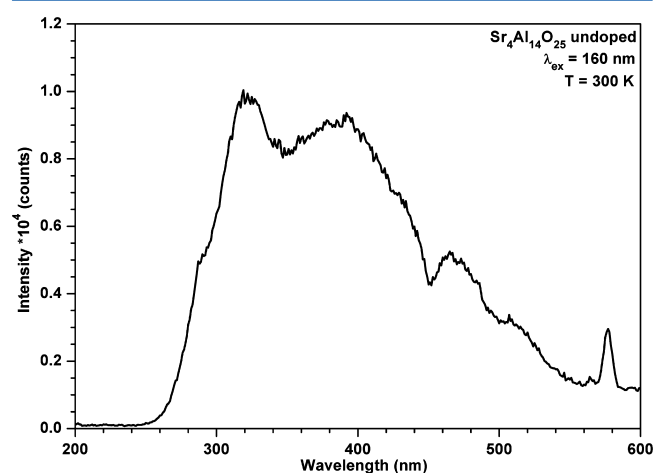


**Figure 1.** Emission spectra of undoped  $\text{Sr}_4\text{Al}_{14}\text{O}_{25}$  excited at 160 nm, recorded at 300 K.

broad emission band between 260 and 550 nm with low intensity. Since there is no evidence for any rare earth ion impurity or other luminescent ions, the structured emission band points to the presence of several different luminescent defect states in the material, e.g., oxygen vacancies, commonly observed in oxides.

The UV excited emission spectra of  $\text{Sr}_4\text{Al}_{14}\text{O}_{25}:0.1\%\text{Eu}^{2+}$  at room temperature and at 4 K are presented in Figure 2. At room temperature the emission spectrum consists of two bands peaking at 425 and 490 nm. On the basis of covalency and crystal field arguments, the high energy 425 nm emission band of  $\text{Eu}^{2+}$  can be assigned to  $\text{Eu}^{2+}$  on the 10-fold coordinated site and the low energy 490 nm band to the 7-fold coordinated site.<sup>3,4,6,9</sup> The emission spectra change strongly with temperature. Upon decreasing temperature to 4 K, the 425 nm emission band shifts to 400 nm. The blue shift of the high energy  $\text{Eu}^{2+}$  emission band is in agreement with previous observations in the literature, where it was however not explained.<sup>9</sup> The 490 nm emission band does hardly shift and shows the commonly observed narrowing upon cooling. In addition, some weak and sharp emission lines are observed around 585 and 615 nm (insert Figure 2). These sharp emission lines are assigned to  $^5\text{D}_0 \rightarrow ^7\text{F}_1$  and  $^5\text{D}_0 \rightarrow ^7\text{F}_2$  transitions of  $\text{Eu}^{3+}$ , which is present in trace amounts. The

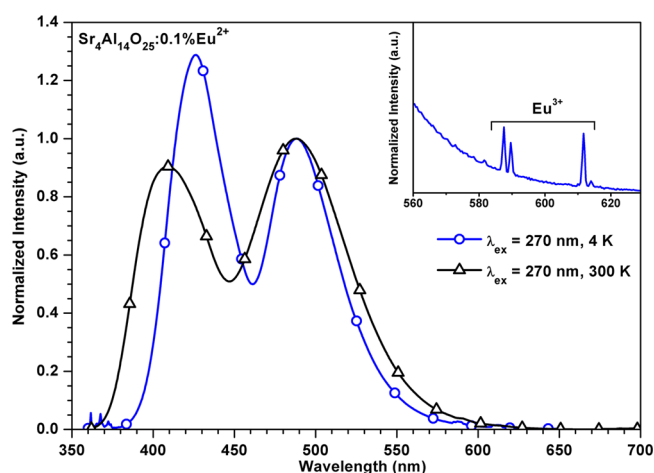


**Figure 2.** Emission spectra of  $\text{Sr}_4\text{Al}_{14}\text{O}_{25}:0.1\%\text{Eu}^{2+}$  for excitation at 270 nm at 4 and 300 K. The inset shows an enlarged spectrum in the 560–630 nm range with emission lines assigned to traces of  $\text{Eu}^{3+}$ .

presence of  $\text{Eu}^{3+}$  is peculiar since the material has been synthesized under strongly reducing conditions. It seems to be a characteristic that is typical for efficient  $\text{Eu}^{2+}$  doped afterglow materials. In the low temperature emission spectrum, very weak lines are observed around 360 nm. These may correspond to intraconfigurational  $4f^7$  transitions ( $^6\text{P}_{7/2} \rightarrow ^8\text{S}_{7/2}$ ) for  $\text{Eu}^{2+}$  in a small amount (below the XRD detection limit) of  $\text{SrAl}_{12}\text{O}_{19}$ .

To get further insight in the origin of the blue shift, a systematic study on  $\text{Sr}_4\text{Al}_{14}\text{O}_{25}:\text{Eu}^{2+}$  was performed as a function of the temperature. Emission spectra were measured between 100 and 500 K, and a selection of these spectra is presented in Figure 3. The spectra show a small and gradual

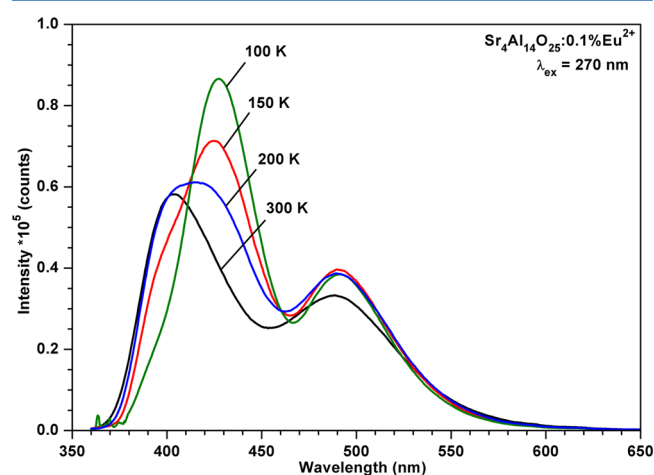


**Figure 3.** Emission spectra of  $\text{Sr}_4\text{Al}_{14}\text{O}_{25}:0.1\%\text{Eu}^{2+}$  for 270 nm excitation recorded at 100, 150, 200, and 300 K.

blue shift for the 490 nm emission band, as well as some temperature induced broadening, which is commonly observed for  $\text{Eu}^{2+}$  d–f emission. The short wavelength emission band shows a gradual change from the 425 nm emission to 400 nm emission. At 100 K, the 425 nm band dominates. At 150 K, a shoulder develops at the short wavelength side, which increases in intensity with temperature. At 200 K, the two bands have approximately equal intensities, and at 300 K, the 400 nm band dominates. These observations indicate that the two emission bands originate from different states of the same  $\text{Eu}^{2+}$  center.

Excitation spectra for the different emission bands in  $\text{Sr}_4\text{Al}_{14}\text{O}_{25}:0.1\% \text{Eu}^{2+}$  are shown in Figure 4. The spectrum

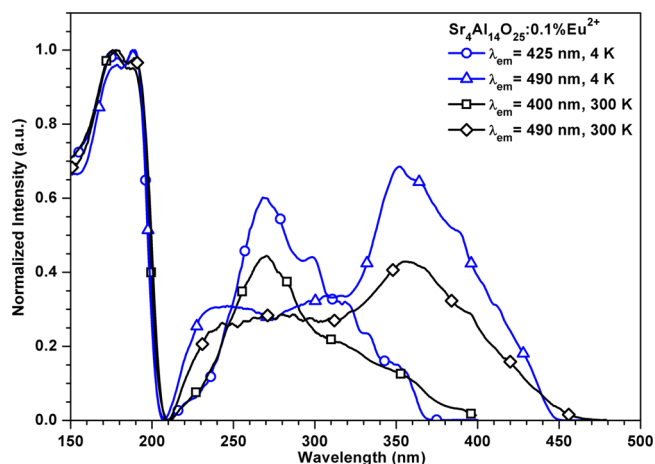


**Figure 4.** Excitation spectra of the  $\text{Eu}^{2+}$  emission in  $\text{Sr}_4\text{Al}_{14}\text{O}_{25}:0.1\% \text{Eu}^{2+}$  at 4 and 300 K for the 400, 425, and 490 nm emission.

recorded for 490 nm emission consists of a broad band ranging from 210 to 460 nm with its maximum at 360 nm. The excitation spectra recorded for 400 and 425 nm emission have very similar shapes and positions of the maxima (at 280 nm). The similarity confirms that the 400 and 425 nm emission bands originate from the same  $\text{Eu}^{2+}$  center. Note that the small differences can be explained by the difference in temperature. The excitation spectrum for the 425 nm emission is recorded at 4 K and shows a sharp onset at 370 nm, while the excitation spectrum for the 425 nm emission is recorded at 300 K and shows thermal broadening at the onset. The difference between the excitation spectra for the 490 nm emission and the 400/425 nm emission shows that these emission bands originate from different  $\text{Eu}^{2+}$  centers. A sharp edge at about 200 nm (6.2 eV) can be observed in the excitation spectrum of all three emission bands. This onset is assigned to the fundamental absorption edge of the aluminate host lattice. The observation of the host absorption at exactly the same energy for all three emissions indicates that the emission bands are all due to  $\text{Eu}^{2+}$  in the  $\text{Sr}_4\text{Al}_{14}\text{O}_{25}$  host and excludes emission from  $\text{Eu}^{2+}$  in impurity phases.

The broad excitation band of the 490 nm emission overlaps with both the 400 and 425 nm emission bands causing energy transfer to  $\text{Eu}^{2+}$  ions emitting 490 nm, as observed in the literature to be very efficient already at 0.5 and 1% of  $\text{Eu}^{2+}$ .<sup>9,15</sup> It can also be observed that the spectral overlap is larger for the 400 nm emission than for the 425 nm emission band, and consequently, energy transfer is expected to become more efficient upon raising the temperature. To obtain a more quantitative estimate of the relative intensities of the three emission bands, the spectra were fitted using three Gaussian profiles for emission spectra recorded under 270 nm excitation where both  $\text{Eu}^{2+}$  centers absorb. The relative areas of the three different emission bands are plotted as a function of temperature in Figure 5. An anticorrelation in intensity between the two bands at 400 and 425 nm can be observed at low temperatures (below 300 K). Thermal quenching of all bands occurs above 300 K. The room temperature emission spectrum consists mainly of the 400 and 490 nm emission bands. It can be also observed that the intensity of the emission at 490 nm increases with temperature between 100 and 250 K, together

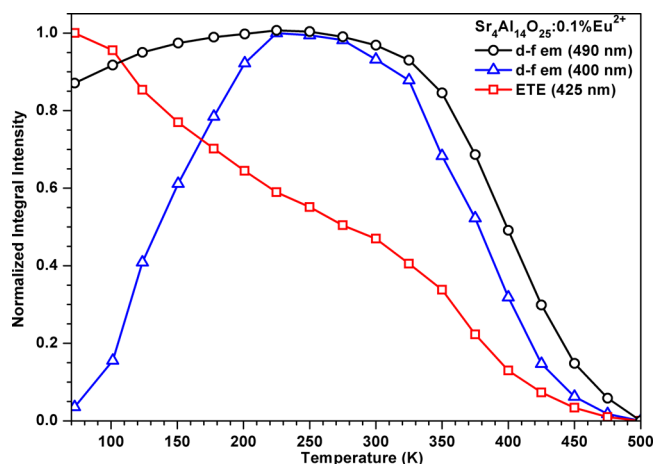


**Figure 5.** Luminescence intensity of the three different emission bands (400, 425, and 490 nm) of  $\text{Sr}_4\text{Al}_{14}\text{O}_{25}:0.1\% \text{Eu}^{2+}$  under 270 nm excitation as a function of temperature.

with the increase of the 400 nm emission band. This behavior can be explained by more efficient energy transfer due to the transition from the 425 to the 400 nm emission, which increases the spectral overlap for energy transfer.

Finally, luminescence lifetime measurements were performed for the different emission bands at different temperatures for excitation at 265 or 375 nm. The results are shown in Figure 6. The emission at 490 nm shows a single exponential behavior with a lifetime of 0.94  $\mu\text{s}$  at 100 K, which decreases slightly to 0.83  $\mu\text{s}$  at 300 K, which is explained by the onset of thermal quenching around 300 K for the  $\text{Eu}^{2+}$  emission. The decay time of almost 1  $\mu\text{s}$  is characteristic for  $4f^65d^1-4f^7$  emission of  $\text{Eu}^{2+}$  around 490 nm.<sup>16</sup> The shortening observed in the decay time of 490 nm emission with increasing temperature is caused by thermal quenching, which starts around 300 K (see Figure 3). The high energy emission bands at 400 or 425 nm show a close to single exponential decay at low temperatures, and the lifetimes are shorter than those for the 490 nm emission. The decay times measured for the emission at 400 and 425 nm are similar, around 0.51  $\mu\text{s}$  at 100 K. At 300 K, the decay time has shortened to 0.24  $\mu\text{s}$ , while the decay curve has become nonexponential.

The luminescence life times are collected in Table 1. The experimental error is estimated to be  $\sim 0.05 \mu\text{s}$  based on variation in decay times obtained if a different time window is chosen for analysis of the decay time. The similarity of the decay curves for the 400 and 425 nm emission bands is consistent with both emission bands originating from the same luminescent center. Two different excited states in thermal equilibrium will give rise to the same luminescence decay times for emission from both states.

To explain the observations for the 400 and 425 nm emission bands, we assign the emission at 425 nm to anomalous  $\text{Eu}^{2+}$  trapped exciton (ETE) emission and the 400 nm emission to normal  $4f^65d^1-4f^7$  emission. The peculiar shift of the 425 nm emission band with temperature can be explained by temperature induced transition from  $\text{Eu}^{2+}$  trapped exciton to  $4f^65d$   $\text{Eu}^{2+}$  emission. Mostly for  $\text{Eu}^{2+}$   $4f^65d$  emission is observed, but ETE emission has been reported in a variety of host lattices.<sup>16–19</sup> The observation of ETE has been reviewed by Dorenbos<sup>20</sup> and is characterized by a large Stokes shift and low quenching temperature. It is observed more frequently for  $\text{Eu}^{2+}$  on sites with a high coordination number.<sup>20</sup> The ETE is



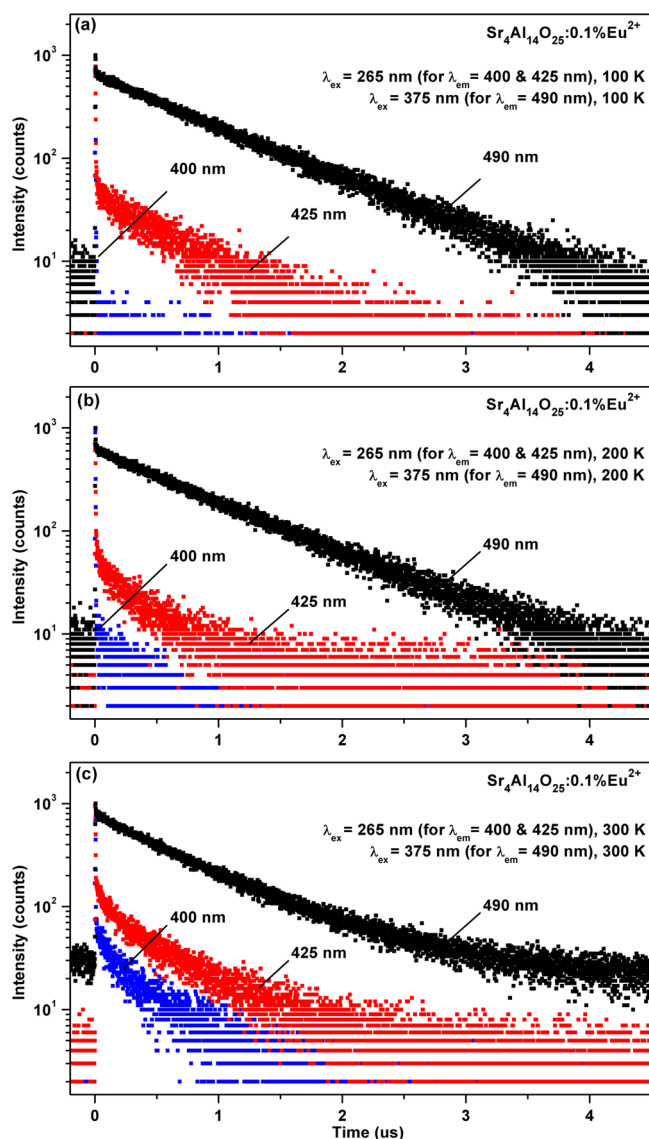


**Figure 6.** Luminescence decay curves of different emission bands (400, 425, and 490 nm) of  $\text{Sr}_4\text{Al}_{14}\text{O}_{25}:0.1\%\text{Eu}^{2+}$  after pulsed excitation (265 or 375 nm) at 100, 200, and 300 K.

**Table 1.** Decay Times  $\tau_{1/e}$  of the 400, 425, and 490 nm Emission Bands Measured at 100 and 300 K for  $\text{Sr}_4\text{Al}_{14}\text{O}_{25}:0.1\%\text{Eu}^{2+}$ ; Typical Uncertainties in the Reported Decay Times Are 0.05  $\mu\text{s}$

| temperature | 400 nm emission band ( $\mu\text{s}$ ) | 425 nm emission band ( $\mu\text{s}$ ) | 490 nm emission band ( $\mu\text{s}$ ) |
|-------------|--|--|--|
| 100 K       |  | 0.52                                   | 0.94                                   |
| 300 K       | 0.24                                   | 0.24                                   | 0.83                                   |

described as a state in which the  $\text{Eu}^{2+}$  ion is ionized to  $\text{Eu}^{3+}$  and the electron is stabilized in the vicinity by delocalization over the neighboring cations.<sup>16–20</sup> If the crystal field splitting for the 5d state is small (e.g., due to a high coordination number) the ETE state can be situated below the  $4f^65d$  state and ETE emission occurs. The most famous example is  $\text{BaF}_2:\text{Eu}^{2+}$ , which shows a broad yellow ETE emission band at low temperatures.<sup>18</sup> Other examples include  $\text{BaS}:\text{Eu}^{2+}$ ,<sup>19</sup>  $\text{CsMgPO}_4:\text{Eu}^{2+}$ ,<sup>17</sup>  $\text{BaSiO}_3$ , and  $\text{Ba}_2\text{Si}_2\text{O}_5$ .<sup>16</sup> In these systems, ETE emission is observed at low temperatures and upon raising the temper-

ature, luminescence quenching of the ETE occurs. In many of the systems showing ETE emission the lowest  $4f^65d$  band is considered to be situated in the conduction band.

In the present case for the 10-coordinated site in  $\text{Sr}_4\text{Al}_{14}\text{O}_{25}:\text{Eu}^{2+}$  the situation is different. The lowest  $4f^65d$  state is located at a slightly higher energy than the ETE state. A configurational coordinate diagram for both  $\text{Eu}^{2+}$  sites in  $\text{Sr}_4\text{Al}_{14}\text{O}_{25}$  is drawn in Figure 7. For the 10-coordinated site, the

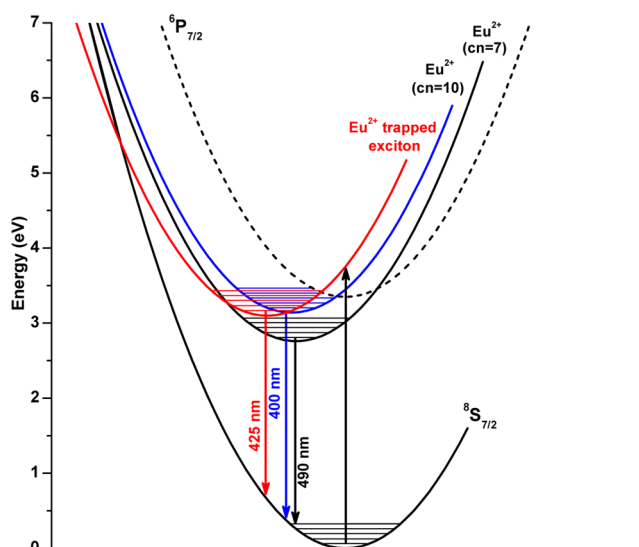


**Figure 7.** Configurational coordinate diagram of  $\text{Eu}^{2+}$  luminescence in  $\text{Sr}_4\text{Al}_{14}\text{O}_{25}$  showing the ground state and excited state for both the 7-coordinated  $\text{Eu}^{2+}$  site (490 nm emission) and the 10-coordinated  $\text{Eu}^{2+}$  site (425 and 400 nm emission).

ETE is slightly lower in energy, and at low temperatures, emission from the ETE state is observed around 425 nm. The Stokes shift for the emission is large,  $\sim 5000\text{ cm}^{-1}$ , as estimated from the energy difference between the lowest energy  $4f^65d$  band ( $\sim 350\text{ nm}$ ) and the emission maximum at 425 nm. This value is large and in the range expected for ETE emission.<sup>20</sup> Note that the Stokes shift determined here is the energy difference between the energy for the lowest energy  $4f^65d$  excitation band and the ETE emission band. This is, in the strict definition, not the Stokes shift, which is defined as the energy difference between the maximum for the excitation and emission band for the same electronic transition. Upon raising the temperature, the  $4f^65d$  state is thermally populated and emission from this state is observed. The energy difference between the ETE and  $4f^65d$  state is small, around  $100\text{ cm}^{-1}$ , as estimated from the increase of the relative intensity of the 400 nm emission band between 100 and 200 K. Above 200 K, the  $4f^65d$  emission dominates. The blue shift from 425 to 400 nm is significantly larger than the  $100\text{ cm}^{-1}$  energy difference. This is due to the much larger relaxation in the ETE excited state than in the  $4f^65d$  excited state. The smaller relaxation for the  $4f^65d$  excited state results in a smaller Stokes shift and thus a higher energy for the emission band maximum. The estimated Stokes shift for the 400 nm  $4f^65d$  emission is  $3600\text{ cm}^{-1}$ , in line with Stokes shifts observed for normal  $4f^65d$  emission from  $\text{Eu}^{2+}$ .<sup>20,21</sup> In the configurational coordinate diagram in Figure 7, the different excited states are depicted for both the 10- and 7-coordinated sites. With this diagram, the luminescence properties and temperature dependence of the  $\text{Eu}^{2+}$  emission in  $\text{Sr}_4\text{Al}_{14}\text{O}_{25}$  can be understood. A transition from ETE

emission to  $4f^65d$  emission has been observed before and can be induced by pressure changes.<sup>22,23</sup> The pressure dependence for the  $4f^65d$  and ETE states is different, and by increasing pressure, a crossing of the  $4f^65d$  state below the ETE state has been demonstrated<sup>23</sup> and explained using a sophisticated model for the pressure dependence of both the  $4f^65d$  and ETE states. The presently observed temperature induced change between ETE and  $4f^65d$  emission has been observed before in  $\text{CsCaF}_3:\text{Eu}^{2+}$  and  $\text{Ba}_{0.3}\text{Sr}_{0.7}\text{F}_2:\text{Eu}^{2+}$ . For  $\text{CsCaF}_3$ , the large temperature induced shift from 610 nm at 300 K to 510 nm at 77 K was recently interpreted by a crossover from ETE to  $4f^65d$  emission.<sup>24</sup> In the mixed fluoride system,  $\text{Ba}_{0.3}\text{Sr}_{0.7}\text{F}_2:\text{Eu}^{2+}$  has been shown that upon raising the temperature a transition from 525 and 430 nm emission occurs, and this was explained by thermal population of a  $4f^65d$  state situated just above the ETE state.<sup>22</sup> Because of the mixed crystal nature, the cation surroundings for different  $\text{Eu}^{2+}$  ions varies in  $\text{Ba}_{0.3}\text{Sr}_{0.7}\text{F}_2:\text{Eu}^{2+}$  giving rise to slightly different energy gaps between the ETE and  $4f^65d$  states. As a result of this inhomogeneity, the transition occurs at different temperatures for different  $\text{Eu}^{2+}$  ions and the luminescence decay curves become nonexponential. For the 10-coordinated site in  $\text{Sr}_4\text{Al}_{14}\text{O}_{25}$ , the energy difference between the  $4f^65d$  and ETE state is the same for all  $\text{Eu}^{2+}$  ions, and we can observe a temperature induced crossover from ETE to  $4f^65d$  emission. The proximity of the two states makes this system also interesting for pressure-dependent measurements.

#### 4. CONCLUSIONS

The luminescence properties of  $\text{Sr}_4\text{Al}_{14}\text{O}_{25}:\text{Eu}^{2+}$  have been investigated as a function of temperature. Because of the low  $\text{Eu}^{2+}$  doping concentration (0.1%) emission from both the 7- and 10-coordinated site can be studied. The long wavelength emission band around 490 nm is assigned to  $4f^65d$  emission from  $\text{Eu}^{2+}$  on the 7-coordinated site and is efficient up to 300 K, the onset for temperature quenching. The luminescence behavior for  $\text{Eu}^{2+}$  on the 10-coordinated site is peculiar and shows a large shift from 425 nm at low temperatures to 400 nm at 300 K. The temperature induced shift is explained by a transition from anomalous  $\text{Eu}^{2+}$  trapped exciton emission to normal  $4f^65d$  emission due to the position of the  $4f^65d$  state just above the ETE state but below the conduction band.

#### AUTHOR INFORMATION

##### Notes

The authors declare no competing financial interest.

#### REFERENCES

- (1) Blasse, G.; Bril, A. Fluorescence of  $\text{Eu}^{2+}$ -Activated Alkaline Earth Aluminates. *Philips Res. Rep.* **1968**, *23*, 201–206.
- (2) Koike, J.; Kojima, T.; Toyonaga, R.; Kagami, A.; Hase, T.; Inaho, S. New Tricolor Phosphors for Gas Discharge Display. *J. Electrochem. Soc.* **1979**, *126*, 1008–1010.
- (3) Smets, B.; Rutten, J.; Hoeks, G.; Verlijdsdonk.  $2\text{SrO} \cdot 3\text{Al}_2\text{O}_3:\text{Eu}^{2+}$  and  $1.29(\text{Ba,Ca})\text{O} \cdot 6\text{Al}_2\text{O}_3:\text{Eu}^{2+}$ : Two New Blue-Emitting Phosphors. *J. Electrochem. Soc.* **1989**, *136*, 2119–2123.
- (4) Wu, Z.; Shi, J.; Wang, J.; Gong, M.; Su, Q. Synthesis And Luminescent Properties of  $\text{Sr}_4\text{Al}_{14}\text{O}_{25}:\text{Eu}^{2+}$  Blue–Green Emitting Phosphor for White Light-Emitting Diodes (Leds). *J. Mater. Sci.: Mater. Electron.* **2008**, *19*, 339–342.
- (5) Aitasalo, T.; Hölsä, J.; Jungner, H.; Lastusaari, M.; Niittykoski, J. Thermoluminescence Study Of Persistent Luminescence Materials:  $\text{Eu}^{2+}$ - And  $\text{R}^{3+}$ -Doped Calcium Aluminates,  $\text{CaAl}_2\text{O}_4:\text{Eu}^{2+}, \text{R}^{3+}$ . *The Journal of Physical Chemistry. B* **2006**, *110*, 4589–4598.

- (6) Lin, Y.; Tang, Z.; Zhang, Z. Preparation of Long-Afterglow Sr Al O-Based Luminescent 4 14 25 Material and Its Optical Properties. *Mater. Lett.* **2001**, *51*, 14–18.
- (7) Lin, Y.; Tang, Z.; Zhang, Z.; Nan, C. W. Anomalous Luminescence in  $\text{Sr}_4\text{Al}_{14}\text{O}_{25}:\text{Eu}$ , Dy Phosphors. *Appl. Phys. Lett.* **2002**, *81*, 996–998.
- (8) Nagamani, S.; Panigrahi, B. S. Luminescence Properties of  $\text{SrO-Al}_2\text{O}_3:\text{Eu}^{2+}, \text{Dy}^{3+}$  Prepared at Different Temperatures. *J. Am. Ceram. Soc.* **2010**, *93*, 3832–3836.
- (9) Nakazawa, E.; Murazaki, Y.; Saito, S. Mechanism of the Persistent Phosphorescence in  $\text{Sr}_4\text{Al}_{14}\text{O}_{25}:\text{Eu}$  and  $\text{SrAl}_2\text{O}_4:\text{Eu}$  Codoped with Rare Earth Ions. *J. Appl. Phys.* **2006**, *100*, 113113.
- (10) Yuan, Z.-X.; Chang, C.-K.; Mao, D.-L.; Ying, W. Effect of Composition on the Luminescent Properties of  $\text{Sr}_4\text{Al}_{14}\text{O}_{25}:\text{Eu}^{2+}, \text{Dy}^{3+}$  Phosphors. *J. Alloys Compd.* **2004**, *377*, 268–271.
- (11) Zych, A.; Leferink op Reinink, A.; van der Eerden, K.; de Mello Donegá, C.; Meijerink, A. Luminescence Properties of Lanthanide Doped Alkaline Earth Chlorides Under (V)UV and X-Ray Excitation. *J. Alloys Compd.* **2011**, *509*, 4445–4451.
- (12) Li, Q.; Zhao, J.; Sun, F. Energy Transfer Mechanism of  $\text{Sr}_4\text{Al}_{14}\text{O}_{25}:\text{Eu}^{2+}$  Phosphor. *J. Rare Earths* **2010**, *28*, 26–29.
- (13) Capron, M.; Fayon, F.; Massiot, D.; Douy, A.  $\text{Sr}_4\text{Al}_{14}\text{O}_{25}$ : Formation, Stability, and Al-27 High-Resolution NMR Characterization. *Chem. Mater.* **2003**, *15*, 575–579.
- (14) Zhao, C.; Chen, D.; Yuan, Y.; Wu, M. Synthesis of  $\text{Sr}_4\text{Al}_{14}\text{O}_{25}:\text{Eu}^{2+}, \text{Dy}^{3+}$  Phosphor Nanometer Powders by Combustion Processes and its Optical Properties. *Mater. Sci. Eng., B* **2006**, *133*, 200–204.
- (15) Peng, M.; Pei, Z.; Hong, G.; Su, Q. Study on the Reduction of  $\text{Eu}^{3+} \rightarrow \text{Eu}^{2+}$  in  $\text{Sr}_4\text{Al}_{14}\text{O}_{25}:\text{Eu}$  Prepared in Air Atmosphere. *Chem. Phys. Lett.* **2003**, *371*, 1–6.
- (16) Poort, S. H. M.; Meijerink, A.; Blasse, G. Lifetime Measurements in  $\text{Eu}^{2+}$ -Doped Host Lattices. *J. Phys. Chem. Solids* **1997**, *58*, 1451–1456.
- (17) Huang, Y.; Seo, H. J. Luminescence of  $\text{Eu}^{2+}$  Ions in  $\text{CsMgPO}_4$  Phosphor: Anomalous Emission and its Origin. *J. Electrochem. Soc.* **2011**, *158*, J260–J263.
- (18) Moine, B.; Pedrini, C.; Courtois, B. Photoionization and Luminescences in  $\text{BaF}_2:\text{Eu}^{2+}$ . *J. Lumin.* **1991**, *50*, 31–38.
- (19) Smet, P. F.; Van Haecke, J. E.; Loncke, F.; Vrielinck, H.; Callens, F.; Poelman, D. Anomalous Photoluminescence in  $\text{BaS}:\text{Eu}$ . *Phys. Rev. B* **2006**, *74*, 035207.
- (20) Dorenbos, P. Anomalous Luminescence of  $\text{Eu}^{2+}$  and  $\text{Yb}^{2+}$  in Inorganic Compounds. *J. Phys.: Condens. Matter* **2003**, *15*, 2645–2665.
- (21) Dorenbos, P. Energy of the First  $4f(7) \rightarrow 4f(6)5d$  Transition of  $\text{Eu}^{2+}$  in Inorganic Compounds. *J. Lumin.* **2003**, *104*, 239–260.
- (22) Mahlik, S.; Wiśniewski, K.; Grinberg, M.; Meltzer, R. S. Temperature and Pressure Dependence of the Luminescence of  $\text{Eu}^{2+}$ -Doped Fluoride Crystals  $\text{Ba}_x\text{Sr}_{1-x}\text{F}_2$  ( $x = 0, 0.3, 0.5$  and 1): Experiment and Model. *J. Phys.: Condens. Matter* **2009**, *21*, 245601.
- (23) Mahlik, S.; Wisniewski, K.; Grinberg, M.; Seo, H. J. Luminescence of  $\text{LiBaF}_3$  and  $\text{KMgF}_3$  Doped with  $\text{Eu}^{2+}$ . *J. Non-Cryst. Solids* **2010**, *356*, 1888–1892.
- (24) Happek, U.; Aycibin, M.; Srivastava, A. M.; Comanzo, H. A.; Camardello, S. On the Luminescence of Octahedrally Coordinated  $\text{Eu}^{2+}$  in  $\text{CsCaF}_3$ . *ECS Trans.* **2009**, *25*, 39–43.